Electronic Supplementary Information

Highly Selective Electrocatalytic Reduction of Nitrate to Ammonia over Copper-Cobalt bimetallic catalyst

Daopeng Li,[a,b] Shengbo Zhang,*[a,b] ZhixianMao,[a,b] Min Liu,[a] Kui Hu,[a] Dongnan Zhao,[a] Zhengguo Qv,[a] Li Zhou,[a] TongfeiShi*[a,b]

[a]Key Laboratory of Materials Physics, Centre for Environmental and Energy Nanomaterials, Anhui Key Laboratory of Nanomaterials and Nanotechnology, CAS Center for Excellence in Nanoscience Institute of Solid State Physics, HFIPS, Chinese Academy of Sciences, Hefei 230031, China

[b] University of Science and Technology of China, Hefei 230026, China

* Corresponding author: E-mail: tfshi@issp.ac.cn; shbzhang@issp.ac.cn

1. Experimental Section

1.1. Chemicals and materials

K_2SO_4 (99.0%), KNO_3 (99.0%), sodium nitroferricyanide(III) dehydrate ($C_5FeN_6Na_2O·2H_2O$, 99.0%), sodium citrate ($C_6H_5Na_3O_7·2H_2O$, 99.0%), NaOH (96.0%), salicylic acid ($C_7H_6O_3$, 99.5%), NaClO (available chlorine ≥ 5.0%), NH_4Cl (99.5%), paminobenzenesuifonamide ($NH_2C_6H_4SO_2NH_2$, 95.0%), N-(1-naphthyl) ethylenediamine dihydrochloride ($C_{10}H_7NHC_2H_4NH_2·2HCl$, 95.0%), $^{15}KNO_3$ (AR), $^{14}NH_4Cl$ (AR), $^{15}NH_4Cl$ (AR),urea, were purchased from Shanghai Aladdin Biochemical Technology Co., Ltd. Shanghai. All solutions were prepared using deionized water (Millipore Corp., 18.2 MΩ cm). Commercial carbon paper (CP, HCP030N) was purchased from Shanghai Hesen Electric Co. Ltd.

1.2. Synthesis of Cu-Co/BPC

Preparation of Metal Ion Solution: A solution was prepared by dissolving 7 mmol of copper (II) nitrate hexahydrate ($Cu(NO_3)_2·6H_2O$), 1 mmol of cobalt(II) nitrate hexahydrate ($Co(NO_3)_2·6H_2O$), and 0.3 g of urea in 25 mL of distilled water.

Incorporation of Co conut Powder: To this solution, 1 g of coconut powder was added and the mixture was continuously stirred for 24 hours. This process yielded urea-treated coconut powder infused with copper and cobalt.

Hydrothermal Treatment: The resulting mixture was then transferred into a 50 mL hydrothermal reactor and treated at 160°C for 14 hours.

Filtration and Drying: The product obtained after hydrothermal treatment was filtered and subsequently dried at 60°C for 10 hours.

Thermal Treatment: The dried material was subjected to thermal treatment in a tubular furnace at 400°C for 2 hours. The final outcome was a biomass-derived porous carbon material that has been modified with metal composites.

Experimental details of electrochemical tests: We dissolved 2mg of catalyst in 10 μL of nafion117, 490 μL of ethanol, and 500 μL of water, and then dripped 500 μL of the mixed solution onto a 1 cm^2 carbon paper.

1.3. Material characterization

X-ray diffraction (XRD) patterns were acquired using Philips X'pert Super with Cu Ka radiation (λ = 1.5418 Å). The transmission electron microscopy (TEM) images were obtained using JEMARM 200F. The aberration-corrected high-angle annular dark-field scanning transmission electron microscopy (HAADF-STEM) measurements and EDX spectroscopy were performed on a JEM-ARM200F. The X-ray photoelectron spectroscopy (XPS) spectra were obtained using an ESCALAB 250 X-ray photoelectron spectrometer (Thermo, America). Nitrogen adsorption-desorption isotherms were measured using Autosorb-iQ-Cx. The ^{1}H NMR (nuclear magnetic resonance) spectra were obtained using superconducting Fourier transform nuclear magnetic resonance spectrometer (Bruker Avance-400).

1.4. Determination of ammonia.

Concentration of the produced ammonia was spectrophotometrically detected by the indophenol blue method. In detail, 0.05 mL of sample was taken, and then diluted with 9.95 mL of deionized water. Subsequently, 100 μL of oxidizing solution (sodium hypochlorite and sodium hydroxide), 500 μL of colouring solution (Sodium citrate and Salicylic acid) and 100 μL of catalyst solution (Sodium nitroferricyanide(III) dihydrate) were added respectively to the measured sample solution. After the placement of 1 h at room temperature, the absorbance measurements were performed at wavelength of 697.5 nm. The obtained calibration curve was used to calculate the ammonia concentration.

1.5. Determination of ammonia.

$R(NH_3)$ and FE are calculated by the following equations:

$$S_{NH_3} = \frac{\Delta C_{N-NH_3}}{\Delta C_{N-NO_3}}$$

$$R(NH_3)(\mu g h^{-1} cm^{-2}) = \frac{C(NH_4{}^+ - N)(\mu g mL^{-1}) \times V(ml) \times 17}{t(h) \times 14}$$

$$FE(NH_3)(\%) = \frac{8 \times n(NH_3)(mol) \times F}{Q} \times 100\%$$

$R(NO_2^-)$and FE are calculated by the following equations:

$$R(NO_2{}^-)(\mu g h^{-1} cm^{-2}) = \frac{C(NO_2{}^- - N)(\mu g mL^{-1}) \times V(mL) \times 46}{t(h) \times 14}$$

$$FE(NO_2^-)(\%) = \frac{2 \times n(NO_2{}^-)(mol) \times F}{Q} \times 100\%$$

In the above equation, ΔC_{N-NH3} is the generated concentration of N-NH_3, ΔC_{N-NO3-} is the difference in N-NO_3^- concentration before and after electrolysis; $R(NH_3)$ is the yield of NH_3; $R(NO_2^-)$ is the yield of NO_2^-; $C(NO_2^-\text{-}N)$ is the mass concentration of nitrite nitrogen; V is the volume of the electrolyte solution in the electrolytic cell; t is the reaction time of electrochemical NtRR (2h); 14 is the molar mass of N; 17 is the molar mass of NH_3; 46 is the molar mass of NO_2^-; n(NH_3) is the amount of NH_3; $n(NO_2^-)$ is the amount of NO_2^-; F is Faraday's constant (96485.34); and Q is the charge measured at different potentials.

1.6. ^{15}N Isotope Labelling Experiments

The ^{15}N isotope-labeled NO_3^- electrochemical reduction experiments were carried out with $K^{15}NO_3$ (99atom%^{15}N) as the electrolyte in 0.1 M Na_2SO_4 solution, and the whole process was consistent with the electrochemical experiments of $K^{14}NO_3$. The reacted electrolyte solution was passed through a superconducting transform nuclear magnetic resonance spectrometer (BrukerAV-400III) to obtain a nuclear magnetic resonance hydrogen spectrum to verify the source of NH_3.

1.7. The detailed description of the electrochemical characterization methods

Cyclic Voltammetry (CV) is a widely used electrochemical characterization technique that can be employed to study redox reactions on electrode surfaces, electrocatalytic activity, and reaction kinetics, among other aspects. Its fundamental principle involves applying a voltage that changes linearly with time to the electrode and measuring the resulting current to investigate electrochemical reactions. The voltage typically scans back and forth within a certain range, forming a cycle. Based on the shape of the curve, we can determine the reversibility of the electrode reaction, the likelihood of intermediates, phase boundary adsorption, and new phase formation.

The data of CV in the paper: Init E=-0.16 V, High E=-0.16 V, Low E = -2.06 V, Scan Rate=0.01 V/s, Segment = 20, Sample Interval = 0.001 V, Quiet Time = 2s, Sensitivity = 0.1 A/V

Linear Sweep Voltammetry (LSV) is a technique that investigates electrochemical reactions by linearly altering the potential of the working electrode and measuring the corresponding current, thereby studying the relationship between current and potential. By analyzing the peak potential, peak current, and shape of the voltammetric curve, information such as the redox potential of the electrochemical reaction can be inferred. The data of LSV in the paper: Init E = -0.16 V, Final E = -2.06 V Scan Rate = 0.05 V/s, Sample Interval = 0.001 V, Quiet Time = 2s, Sensitivity = 0.1 A/V

Chronoamperometry (i-t) is an electrochemical experimental method that involves applying a constant potential to the working electrode and measuring the change in current over time. It can be combined with ultraviolet-visible (UV-Vis) spectrophotometry to evaluate the performance of electrocatalysts during reactions. Additionally, repeated chronoamperometry tests can be conducted to assess the stability of the catalyst in the reaction.

The data of i-t in the paper: Sample Interval= 0.1s, Run Time=7200s, Quiet Time= 2s Sensitivity=0.1 A/V

1.8. the advantages and disadvantages of the Cu-Co/BPC catalyst

The Cu-Co/BPC catalyst achieves high yields and high selectivity of ammonia through copper-cobalt synergy. However, during the 10-hour NitRR experiment, the performance of the catalyst gradually decreased with the course of the reaction.

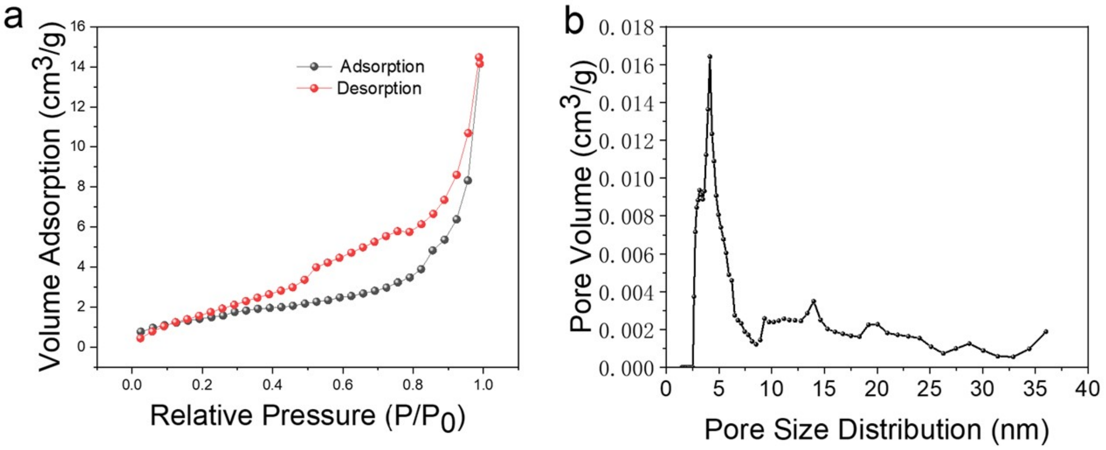

Fig. S1 (a) Nitrogen adsorption and desorption isotherms of Cu-Co/BPC. (b) Pore size distribution curve of Cu-Co/BPC.

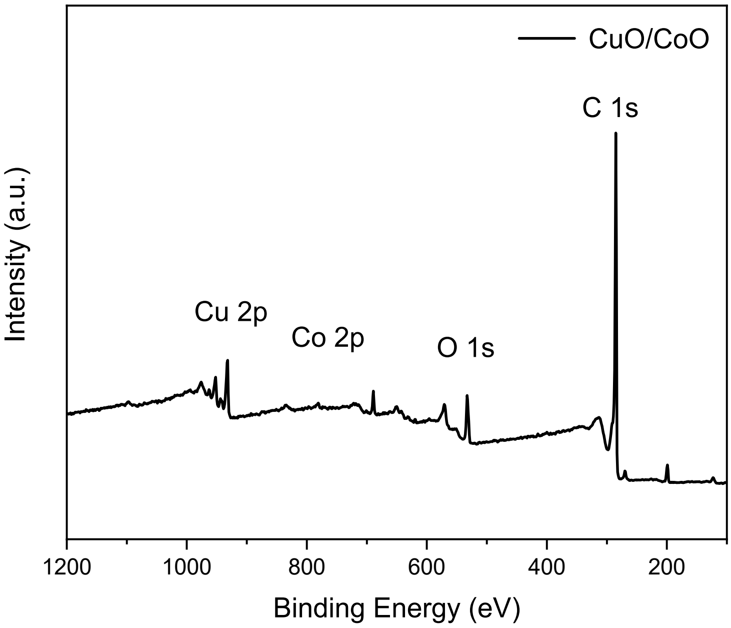

Fig. S2 Survey XPS spectrum of Cu-Co/BPC.

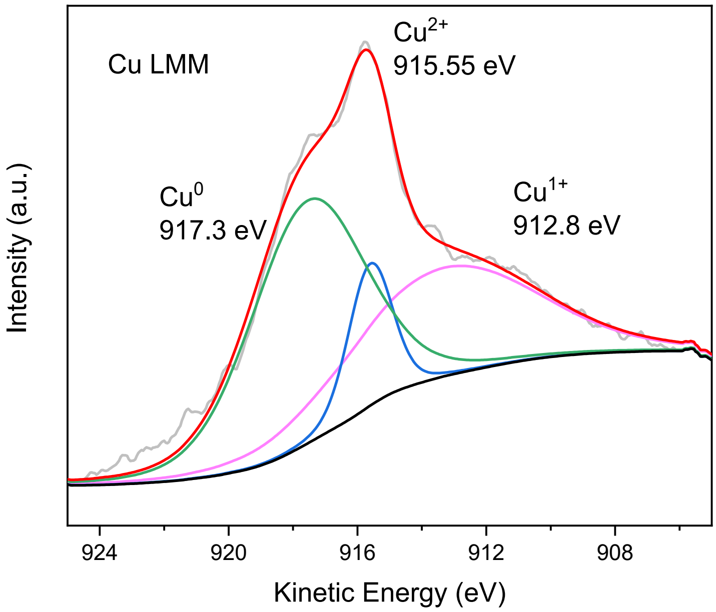

Fig. S3 Cu LMM XPS spectrum of Cu-Co/BPC.

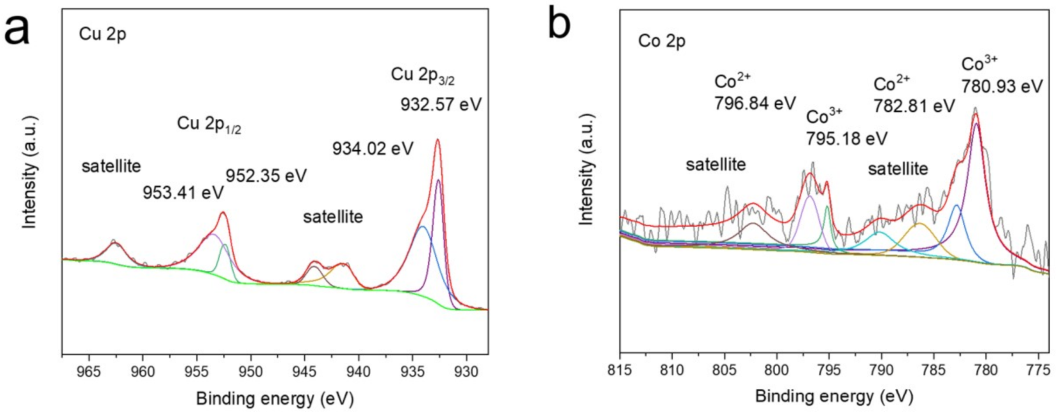

Fig. S4 High-resolution (a) Cu 2p of Cu/BPC, and (b) Co 2p spectra of Co/BPC

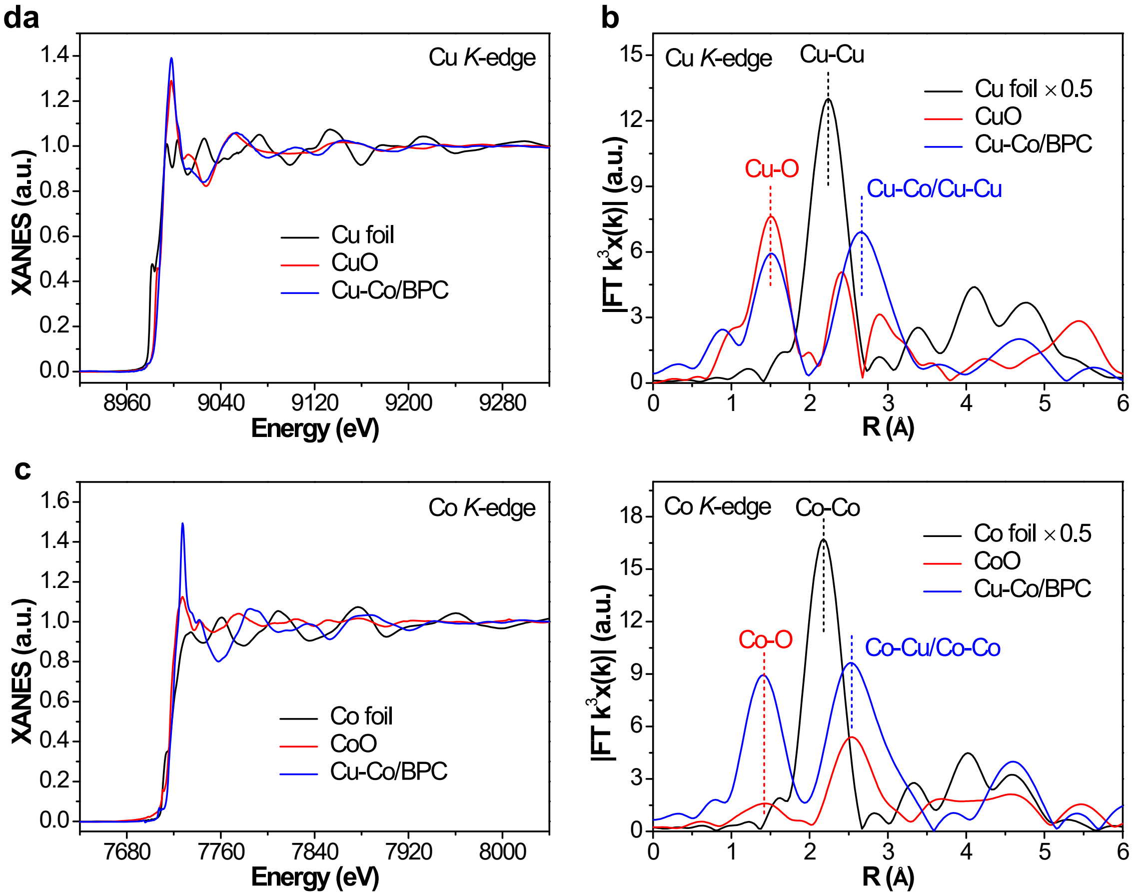

Fig. S5 Cu *K* edge (a) XANES spectra and (b) k^3-weighted FT-EXAFS spectra of Cu-Co/BPC and references, Co *K* edge (c) XANES spectra and (d) k^3-weighted FT-EXAFS spectra of Cu-Co/BPC and references.

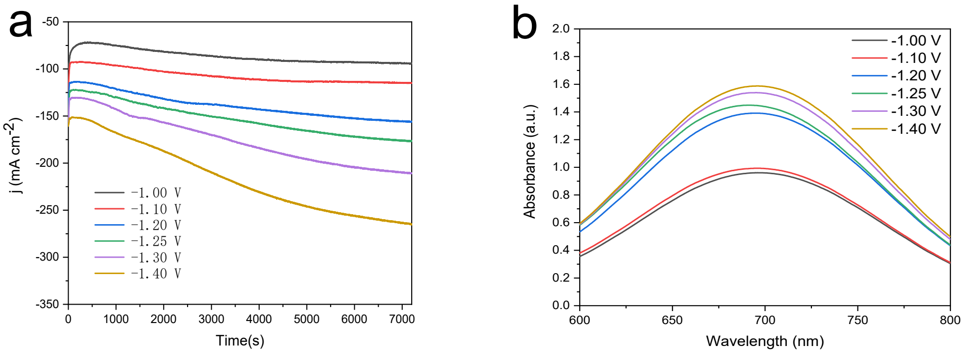

Fig. S6 (a)Time-dependent current density curves at different potentials in 0.1 M N_2SO_4 + 0.1 M N-KNO_3 electrolyte over a 2 h period. (b) UV-Vis absorption spectra obtained from solutions at different potentials.

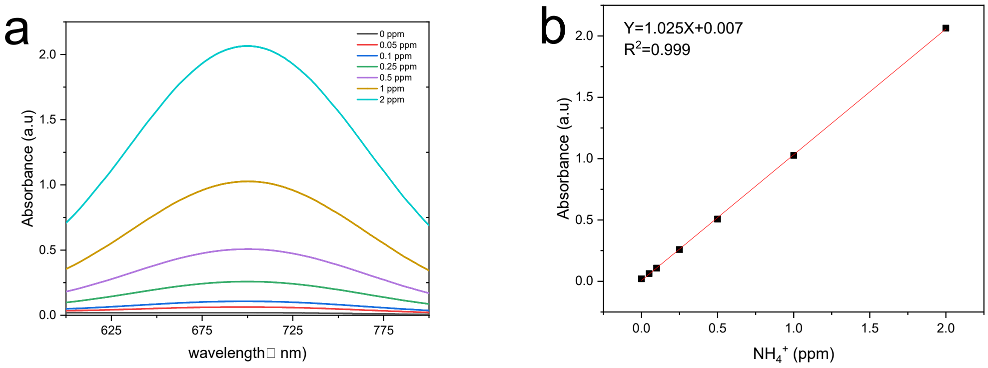

Fig. S7 (a) UV-Vis absorption spectra of various NH_4^+- N concentrations (0, 0.25, 0.50, 0.75, 1, 2 ppm) after incubated for 1 h at room temperature. (b) The calibration curve used for calculation of NH_4^+-N concentration.

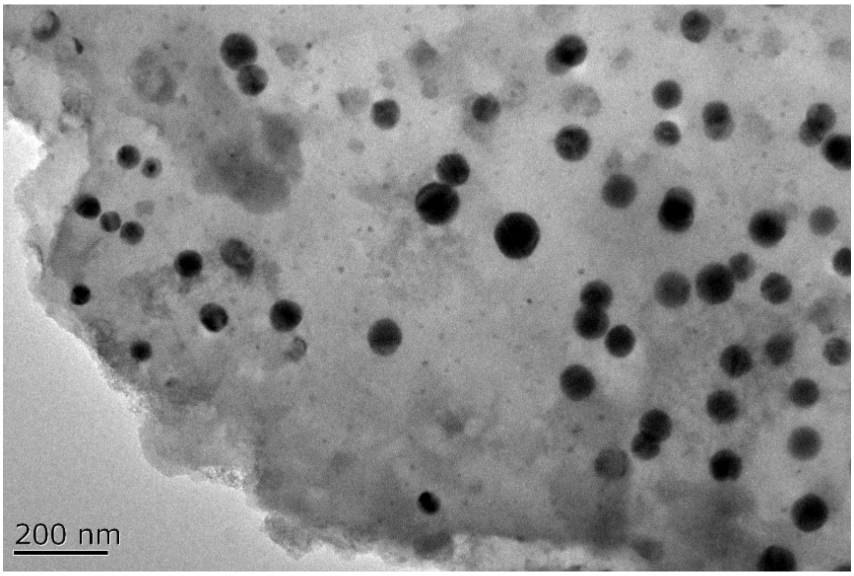

Fig. S8 The TEM image of Cu-Co/BPC after NitRR.

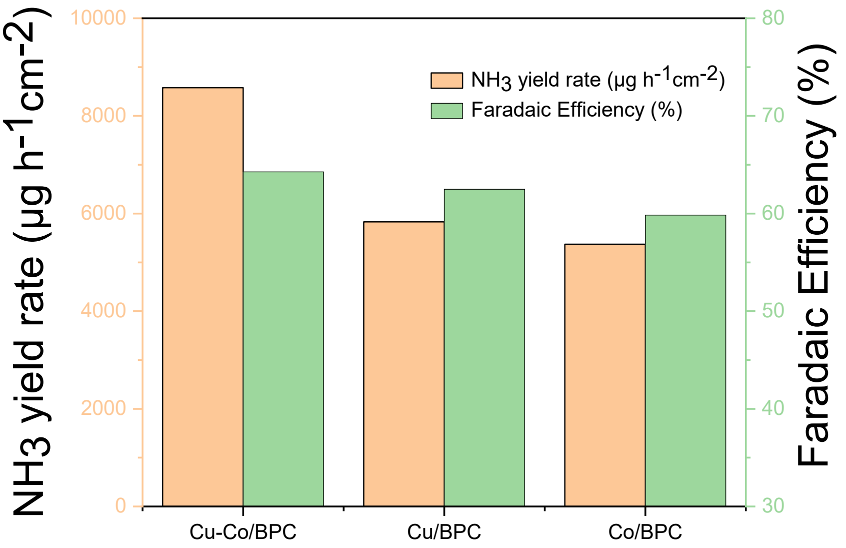

Fig. S9 Performance comparison of Cu/BPC, Co/BPC and Cu Co/BPC.

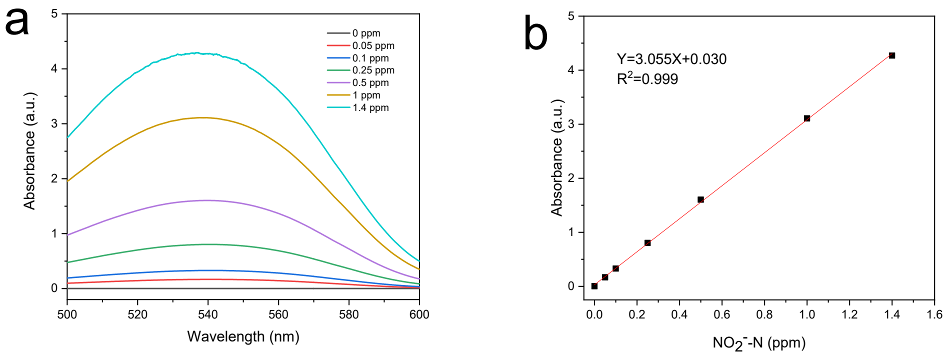

Fig. S10 (a) UV-Vis absorption spectra obtained from the solutions with different NO_2^--N concentrations (0, 0.05, 0.1, 0.25, 0.5, 1,and 1.4 ppm). (b) Calibration curve used to determine NO_2^--N concentration.

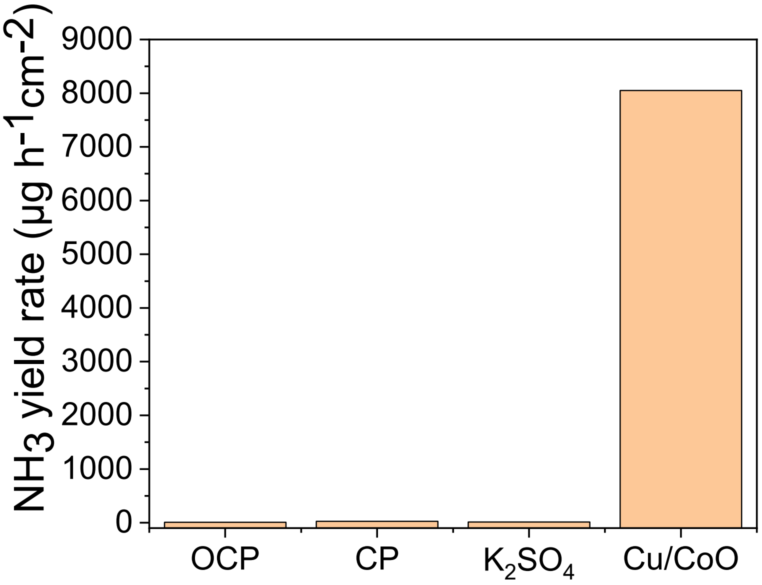

Fig. S11 Controlled experiments under four different conditions.

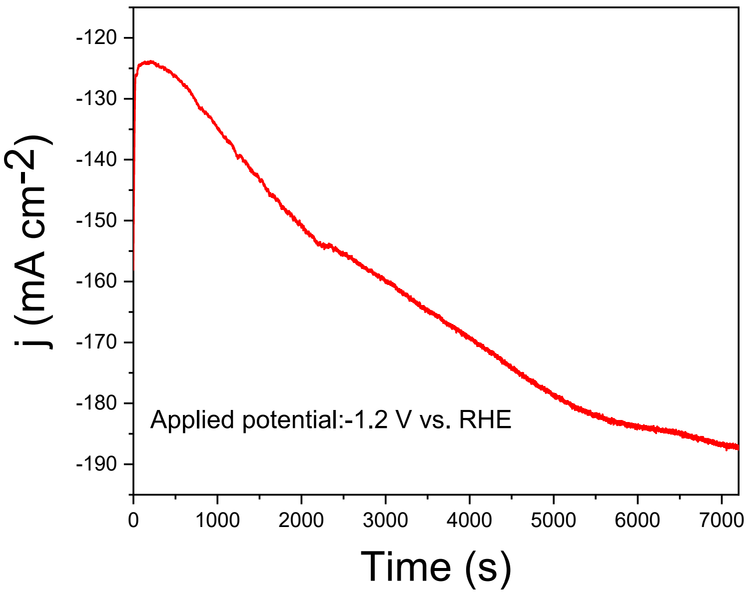

Fig. S12 The time-dependent current change curves of the stability testing.

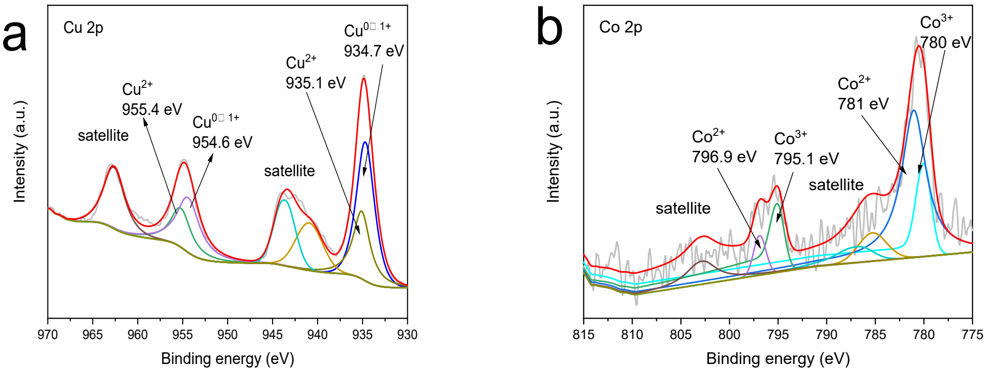

Fig. S13 High-resolution XPS spectra of (a) Cu 2p, (b) Co 2p of Cu-Co/BPC after NitRR with 6 h.

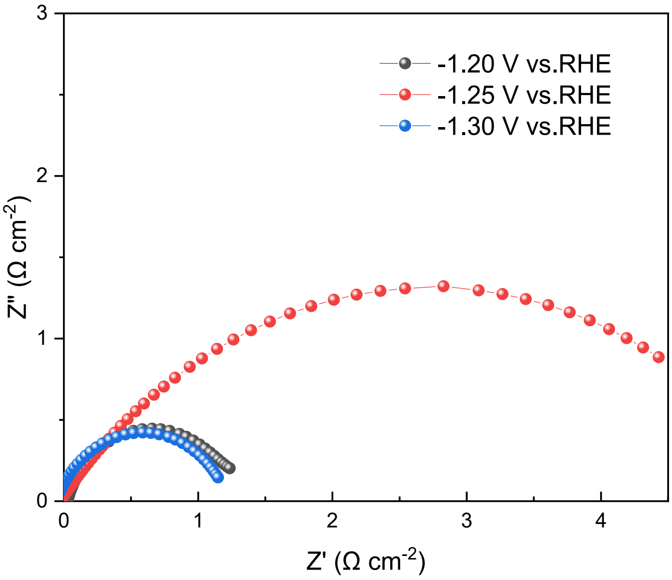

Fig. S14 the electrochemical impedance spectroscopy (EIS) of the catalyst.

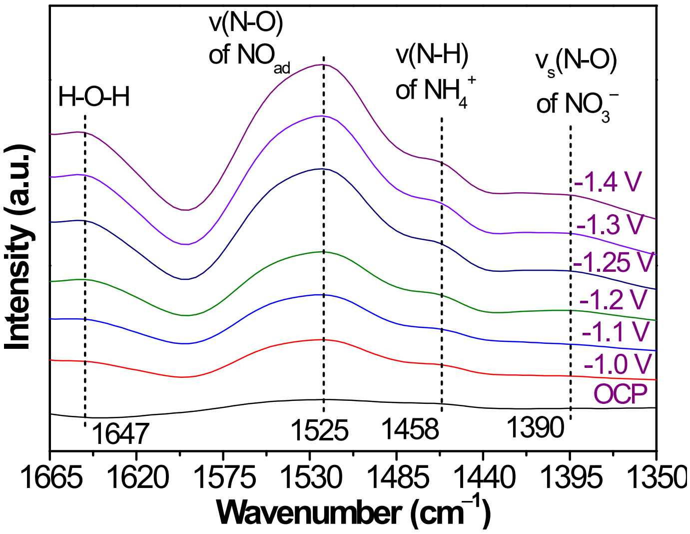

Fig. S15 *In-situ* ATR-SEIRAS spectra of electrocatalytic NitRR on Cu-Co/BPC at different potentials.

Table S1 Comparing the performance of Cu-Co/BPC and other catalysts for the reduction of nitrate to ammonia.

No.	**Catalyst**	**Yield rate**	**FE/%**	**Ref.**
1	CuCoAl LDH /Vulcan	0.22 mol/(h×g)	99.5	1
2	Co/Cu based	1.17 mmol/cm^{-2} h^{-1}	93.3	2
3	$Cu_{50}Ni_{50}$ alloy	0.48 mmol/cm^{-2} h^{-1}	99	3
4	Cu-based MOF	0.00085 mol/(h×g)	10	4
5	Co-based MOF	0.0018 mol/(h×g)	18	4
6	Fe-based MOF	0.001 mol/(h×g)	9	4
7	$Ru_{15}Co_{85}$ HNDs	1.23 mmol/cm^{-2} h^{-1}	96.8	5
8	Co_3O_4/Cu NC	114.0 (mg$_{NH3}$h^{-1} cm^{-2})	97.7	6
9	Cu-Co/BPC	9114.1 μg h^{-1} cm^{-2}	84.5	This Work

references

1. W. Wang, J. Chen and E. C. M. Tse, J. Am. Chem. Soc., 2023, 145, 26678-26687.
2. W. He, J. Zhang, S. Dieckhöfer, S. Varhade, A. C. Brix, A. Lielpetere, S. Seisel, J. R. C. Junqueira and W. Schuhmann, Nat. Commun., 2022, 13, 1129.
3. Y. Wang, A. Xu, Z. Wang, L. Huang, J. Li, F. Li, J. Wicks, M. Luo, D.-H. Nam, C.-S. Tan, Y. Ding, J. Wu, Y. Lum, C.-T. Dinh, D. Sinton, G. Zheng and E. H. Sargent, J. Am. Chem. Soc., 2020, 142, 5702-5708.
4. J. Li, G. Zhan, J. Yang, F. Quan, C. Mao, Y. Liu, B. Wang, F. Lei, L. Li, A. W. M. Chan, L. Xu, Y. Shi, Y. Du, W. Hao, P. K. Wong, J. Wang, S.-X. Dou, L. Zhang and J. C. Yu, J. Am. Chem. Soc., 2020, 142, 7036-7046.
5. S. Han, H. Li, T. Li, F. Chen, R. Yang, Y. Yu and B. Zhang, Nat. Catal., 2023, 6, 402-414.
6. Y. Liu, J. Wei, Z. Yang, L. Zheng, J. Zhao, Z. Song, Y. Zhou, J. Cheng, J. Meng, Z. Geng and J. Zeng, Nat. Commun., 2024, 15, 3619.